Probing the Location of the Terminal Groups of Dendrimers in Dilute Solution

Andreas Topp,[†,§] Barry J. Bauer,[†] June W. Klimash,[‡] Ralph Spindler,[‡] Donald A. Tomalia,[‡] and Eric J. Amis*[,†]

National Institute of Standards and Technology, Gaithersburg, Maryland 20899, and Michigan Molecular Institute, Midland, Michigan 48640

Received January 27, 1999; Revised Manuscript Received July 29, 1999

ABSTRACT: The spatial distribution of the terminal groups of poly(amido amine) dendrimers have been determined experimentally by small-angle neutron scattering with deuterium labeling and scattering contrast variation. The radius of gyration of deuterated terminal units of generation 7 dendrimers is 39.3 ± 1.0 Å. This is significantly larger than the radius of gyration of the whole dendrimer, which is 34.4 ± 0.2 Å. These data indicate that dendrimers have terminal groups that are concentrated near the periphery. These results are inconsistent with many computer simulations and some molecular models.

Introduction

The first dendritic macromolecules with a highly branched and regular architecture were the poly(amido amine) (PAMAM) dendrimers, also called Starburst dendrimers.[1] They are prepared following a divergent approach, with a synthesis consisting of a Michael addition of methyl acrylate to the "core" of ammonia or ethylenediamine, followed by the amidation of the ester function with ethylenediamine (EDA). The repetition of these two reaction steps leads to successive "generations" of the dendrimer. Dendrimers that have primary amines as terminal units are termed "full generations" (G1, G2, ...), while dendrimers terminated at the intermediate synthetic step, with an ester functionality, are referred to as "half-generations" (G0.5, G1.5, ...).

There is a rapidly growing literature reporting a variety of synthetic strategies and chemical pathways to make dendrimers.[2] The majority of these materials have tri- or tetrafunctional cores, and trifunctional branching functionality, as in PAMAM dendrimers. However, the synthetic methods are diverse, as are the resulting chemical structures. Some dendrimers are homogeneous, having a uniform chemical structure throughout, whereas others have more complex structures, such as ones that exhibit ion-chelating capabilities, have an optically active core, or bear electric charges in their structure. The PAMAM dendrimers that we consider here have a complex but uniform building block, with hydrophilic primary amines as terminal groups.

In the pioneering theoretical work on dendritic structures, de Gennes and Hervet predicted a limiting generation for the divergent growth of dendrimers, due to packing arguments.[3] The existence of such a limit and its dependence on the functionality of the core and the spacer length is generally accepted as inherent in the dendritic structure.[2] In the de Gennes model, higher generation dendrimers are pictured as spherical molecules with a low segment density "hollow" interior and with the terminal groups at an outer "surface" of the molecule. Computer simulations, molecular dynamics, Monte Carlo, or kinetic growth modeling provide further predictions for segment density distributions.

In the molecular dynamics simulations, the overall dendrimer shape shows a transition around G2−G4 from an open ellipsoidal structure to a dense packed spherical objects at higher generation.[4,5] In the kinetic growth study by Lescanec and Muthukumar[6] and the Monte Carlo simulation by Mansfield and Klushin,[7,8] segment density profiles are obtained, but an intriguing result is that the terminal groups were seen to be distributed throughout the interior of the dendrimer. Further refined Monte Carlo simulations by Mansfield also show a strong segregation of individual dendrons.

Dendron segregation was also observed in a molecular dynamics study by Murat and Grest, who further described a moderate dependence of the dendrimer dimensions on the solvent quality, a rather uniform segment density distribution in the interior of the dendrimer, and a distribution of the terminal units throughout the molecule.[6−9] The results of Monte Carlo simulations by Chen and Cui[10] are also consistent with these findings, but not by a study reported by Carl.[11] In a self-consistent mean-field study, Boris and Rubinstein also found a monotonically decreasing segment distribution with increasing radius and a dispersion of terminal groups throughout the molecular interior.[12]

Experimental characterization of PAMAM dendrimers by intrinsic viscosity, size exclusion chromatography, and transmission electron microscopy generally suggests that high generations transition to a spherical shape. For example, the intrinsic viscosity exhibits a maximum around G5. The average segment density as calculated from the theoretical molecular weight and hydrodynamic size shows a corresponding minimum at the same generation number.[13,14] Photophysical investigations of PAMAM dendrimers also indicate a transition region for the dendrimer surface that corresponds to an ellipsoid-to-sphere transition as observed in molecular dynamics studies. Higher generation dendrimers exhibit similarities to anionic micelles in the photophysics.[15,16] An experimental investigation of the chain dynamics of small generation PAMAM dendrimers by ^{13}C and ^{2}H NMR relaxation shows very similar relax-

† National Institute of Standards and Technology.
‡ Michigan Molecular Institute.
§ Present address: Continental AG, Materials Research, Hanover, Germany.
* Corresponding author.

10.1021/ma990125s CCC: $18.00
Published on Web 09/28/1999

ation times for the interior segments but shows distinct dynamics of the terminal groups.[17,18]

The most definitive measurements of dendrimer structure come from small-angle neutron scattering (SANS) and small-angle X-ray scattering (SAXS).[19−24] These measurements demonstrate that dendrimers larger than G5 are spherical and have a rather uniform segment density distribution in their interior. Both the uniform segment density and precise molecular dimensions imply that dendrimers represent a unique class of macromolecules.

From theories, simulations, and experimental results, a consistent picture emerges for higher generation dendrimers as spherical molecules with a narrow size distribution, uniform segment density in the interior, and, in general, characteristics of a unimolecular micelle. One critical issue, however, concerns the location and distribution of the terminal units. Despite the importance of the terminal groups for many potential applications, there remains a significant discrepancies for various theoretical studies and simulations. Conclusive experimental results are still lacking.

In this paper, we present results of small-angle neutron scattering experiments with a partially deuterated G7 PAMAM dendrimer, where contrast matching is used to separate the scattering of the terminal groups from that of the whole molecule.

Experimental Section

Sample Preparation. PAMAM dendrimers having a tetrafunctional core of ethylenediamine (EDA) were synthesized according to reported methods.[1,2] Fully hydrogenated G7 PAMAM dendrimers and partially deuterated versions were prepared. The partially deuterated dendrimer was prepared by reacting the fully hydrogeneous G6 dendrimer with partially deuterated methyl acrylate, $CD_2CDCO_2CH_3$ (Cambridge Isotope Laboratories, Andover, MA), to form a G6.5 dendrimer with a hydrogenated interior and deuterated terminal units. The G6.5 was converted to the partially deuterated G7(D) dendrimer by reaction with hydrogenated EDA. The G7(D) therefore is identical to the hydrogenated version G7(H) except that the first half of the final generation is labeled by three deuteriums in each unit. The ^{1}H NMR and ^{13}C NMR spectra of G7(H) and G7(D) agreed with their expected structures, and electophoresis experiments showed similar narrow distribution functions for the two preparations. Methanol solutions were freeze-dried in small vials after addition of four volumes of water. Freeze-dried samples were fluffy white materials, and they were stored only for short periods of time in a dry N_2 atmosphere.

Solutions for small-angle neutron scattering experiments were prepared with methyl alcohol, CH_3OH, and its partially deuterated counterpart, CD_3OH, and used as received (Aldrich Chemical). For the dendrimer concentration series, a master solution of dendrimer in CD_3OH was made, and further dilutions were made to complete the series. For the contrast match determination, two stock solutions of equal G9 dendrimer concentrations were made in CH_3OH and CD_3OH. Various amounts of the two stock solutions were mixed to make a series of solution with different isotopic contents. Once the match point was determined, solutions were made of G7(H) and G7(D) in the match solvent along with G7(H) in CD_3OH. Molar dendrimer concentrations were calculated on the basis of solvent densities $\rho(CH_3OH) = 0.791$ g cm^{-3} and $\rho(CD_3OH) = 0.867$ g cm^{-3} and the theoretical dendrimer molecular weights.[25,26]

Small-Angle Neutron Experiments. Small-angle neutron scattering (SANS) experiments were performed on the 30 m facilities NG3 and NG7 at the Cold Neutron Research Facility (CNRF) of the National Institute of Standards and Technology (Gaithersburg, MD).[27−29] Both instruments were operated at a wavelength of 6 Å and with a wavelength spread $\Delta\lambda/\lambda$ of 0.15. The sample to detector distance was chosen as 610 cm at NG3 and 465 cm at NG7, using a detector offset of 20 and 10 cm, respectively.[30] All experiments were performed at a temperature of 20 °C with a nominal stability of ±0.1 °C.

Two-dimensional scattering data, corrected for detector efficiency, background scattering, and empty cell, were then converted to absolute scattering intensities by use of an H_2O standard and the experimental transmission values. Data were circularly averaged to give the absolute scattering intensity, $I(q)$, as a function of scattering vector q (with $q = (4\pi/\lambda)\sin(\theta/2)$, θ being the scattering angle) with experimental standard deviations of the scattering intensity calculated during the circular averaging using software provided by the CNRF.[31] The dendrimer incoherent scattering was calculated from the hydrogen content of the dendrimers. Incoherent scattering of the solutions was calculated from the composition and subtracted from solution scattering intensities to give the dendrimer coherent scattering intensity.

Results and Discussion

Determination of Radius of Gyration. Partially deuterated methanol, CD_3OH, was chosen for this study because in this solvent we expect no significant electrostatic interactions between the PAMAM dendrimers. In water, the terminating primary amines can become protonated, leading to strong electrostatic interactions in solution. These interations have a strong contribution to the structure factor component of the scattering function and can potentially obscure the apparent radius of gyration of the dendrimers, as determined by scattering.

Partially deuterated methyl alcohol, CD_3OH, was used because the alcoholic proton can exchange with the protons of the terminating primary amines and the internal amido protons. If fully deuterated methyl alcohol were used, i.e., CD_3OD, such exchange of hydrogens with deuteriums would alter the scattering contrast of the deuterium and could change the measured values for R_g. Although we have not observed a measurable influence of this effect in other experiments, use of CD_3OH as the solvent avoids such complications.

Solutions of the G7(H) PAMAM dendrimer in CD_3OH were prepared at molar concentrations, c, of 7×10^{-5}, 3×10^{-5}, and 1×10^{-5} mol dm^{-3}. (The calculation of the molar concentration is based on the theoretical molecular weight of G7(H), $M_t = 1.165 \times 10^5$ g mol^{-1}.) The coherent scattering intensity, I, is shown in Figure 1 as a function of the magnitude of the scattering vector, q. We use the Guinier approximation to determine the radius of gyration of the dendrimers, R_g,

$$\ln I(q) = \ln I(0) - (qR_g)^2/3 \qquad (1)$$

which has been shown to be the appropriate fitting function over this q range for dendrimers.[21−24,32] In this section, the values for the dendrimer radius are indicated as apparent, $R_{g,app}$, since there can be a dependence on concentration for the measured values. As we pointed out in previous reports, this dependence of R_g on c in dilute solutions is a result of contributions to the scattering from the structure factor.[33] This is typical of polymer solutions and should not be misinterpreted as real changes in the dimensions of the dendrimers in these dilute solutions. Linear least-squares fits are shown as solid lines in Figure 1. The similar slopes for different concentrations indicate that the values of $R_{g,app}$ do not vary strongly over this concentration range.

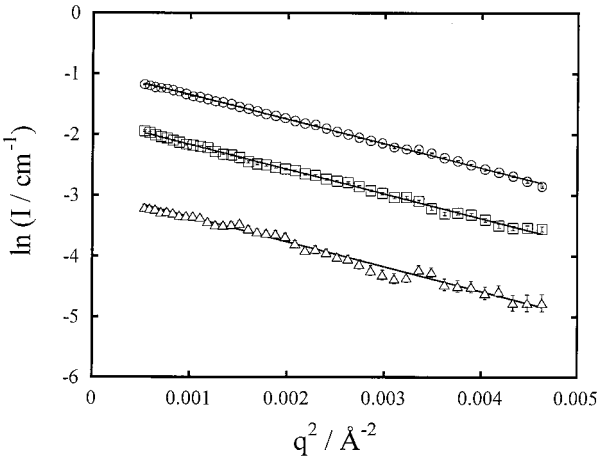

Figure 1. Guinier plot of the scattering intensity of G7(H) in CD_3OH for the following concentrations: (○) $c = 7 \times 10^{-5}$ mol dm^{-3}; (□) $c = 3 \times 10^{-5}$ mol dm^{-3}, (△) $c = 1 \times 10^{-5}$ mol dm^{-3}. The solid lines represent the results of weighted linear least-squares fits to the data. (Uncertainties, plotted as error bars, are calculated on the basis of the experimental standard deviation.)

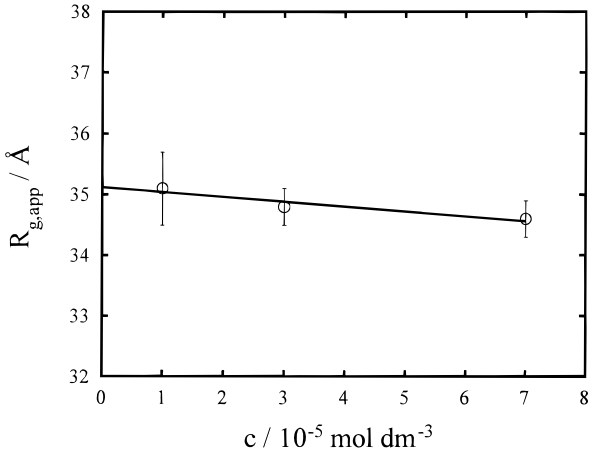

Figure 2. Plot of the apparent radius of gyration, $R_{g,app}$, of G7(H) dendrimer in CD_3OH, calculated from the fits shown in Figure 1, as a function of the dendrimer molar volume concentration. The solid line was obtained from a weighted linear least-squares fit to the data.

Figure 2 shows the values of $R_{g,app}$ with error bars representing one standard deviation as determined from these Guinier fits as a function of c. A weighted linear least-squares extrapolation gives the value of R_g(G7-(H)) = 35.1 ± 0.2 Å. It is clear that the observed concentration dependence of R_g is small over the range of concentrations considered here.

Determination of the Match Point. To isolate the scattering signal of the deuterated parts of the G7(D) dendrimer, the method of contrast matching is used to eliminate contributions from the hydrogenated parts of the molecule. In neutron scattering the intensity is determined by the squared difference of the coherent scattering length of the molecule, b, and the coherent scattering length of the surrounding solvent, a.

The coherent scattering from the molecule vanishes if we adjust the contrast factor of the solvent, a, to have the same value as b.[34] We can accomplish this by using mixtures of deuterated and hydrogenated solvents, in our case mixtures of CD_3OH and CH_3OH. The solvent with composition that leads to $(a - b) = 0$ is a "matching solvent". The composition of this matching solvent is

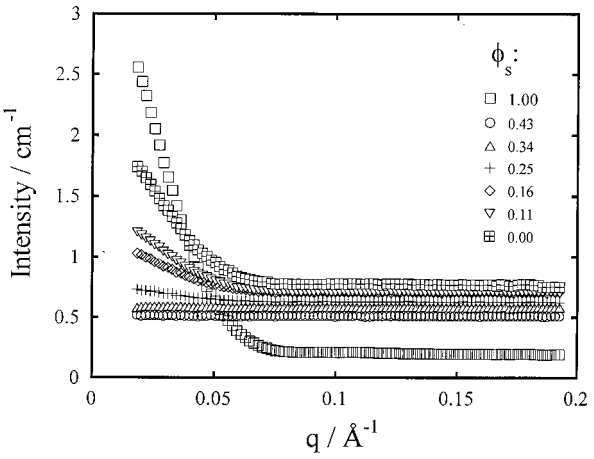

Figure 3. Absolute scattering intensity of solutions of G9 PAMAM dendrimers in solvent mixtures of CD_3OH and CH_3OH for different solvent compositions, ϕ_s, at a constant dendrimer concentration of $c = 4 \times 10^{-5}$ mol dm^{-3}, plotted versus q.

referred to as the "match point", which is characterized by the volume fraction of deuterated solvent in this mixture, ϕ_{match}. When we use a partially deuterated dendrimer in the matching solvent that has the same coherent scattering length as the completely hydrogenated dendrimer, coherent scattering intensity in SANS arises from the deuterated segments of the dendrimer.

The match point for the high-generation PAMAM dendrimer was determined by preparing two stock solutions of the G9 dendrimer in CD_3OH and CH_3OH with a molar volume concentration of $c = 4 \times 10^{-5}$ mol dm^{-3}. Mixtures of the stock solutions with different volume fractions of deuterated solvent, ϕ_s, were measured by SANS. The experimental scattering intensities of these solutions are shown in Figure 3. The amplitude of the coherent scattering intensity has a maximum value for $\phi_s = 1$, disappears at an intermediate value of ϕ_s, and increases again with higher CH_3OH content of the solvent. The incoherent scattering, visible as the high-q value, is a monotonic function proportional to the increasing hydrogen content of the solvent.

The scattering length of the mixed solvent is the average of the scattering lengths of the two components. The total coherent scattering from the mixtures in Figure 3 is proportional to the square of the difference between the solvent composition and the match composition. The coherent scattering of the PAMAM dendrimers in the mixed solvent is estimated from the scattered intensity at $q = 0.02$ Å^{-1}.

The square root of this coherent scattering intensity is plotted in Figure 4 as a function of the solvent composition ϕ_s. Note that the values of $I^{1/2}$ for $\phi_s \geq 0.4$ are plotted negative as expected from predicted magnitude of the solvent and dendrimer scattering cross sections. A linear least-squares fit is used to calculate the match point as $\phi_{match} = 0.388 \pm 0.010$ where the uncertainty is based on one standard deviation from the linear fit.

Location of the Terminal Units. The accuracy of the match point is crucial for these experiments with the partially labeled dendrimers. To verify the matching conditions for the PAMAM dendrimer, a solution of G7-(H) in the matching solvent is prepared at a concentration of $c = 7 \times 10^{-5}$ mol dm^{-3}. Figure 5 shows, on an expanded scale, the absolute scattering intensity of the

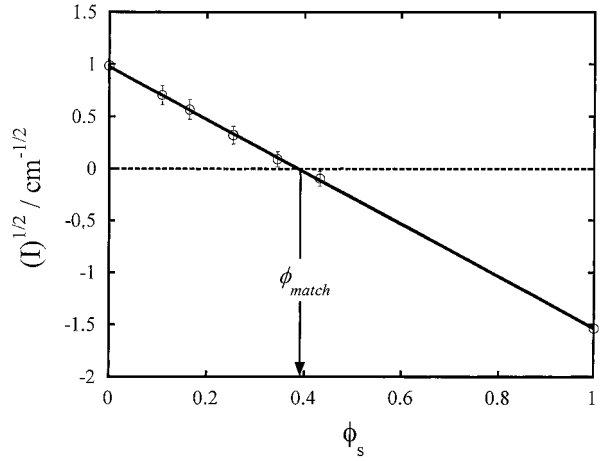

Figure 4. Plot of the square root of the coherent scattering intensities of solutions of G9 PAMAM dendrimer in mixtures of CD_3OH and CH_3OH versus the volume fraction of deuterated solvent, ϕ_s; values of $I^{1/2}$ for $\phi_s \geq 0.4$ are made negative to result in a straight line.

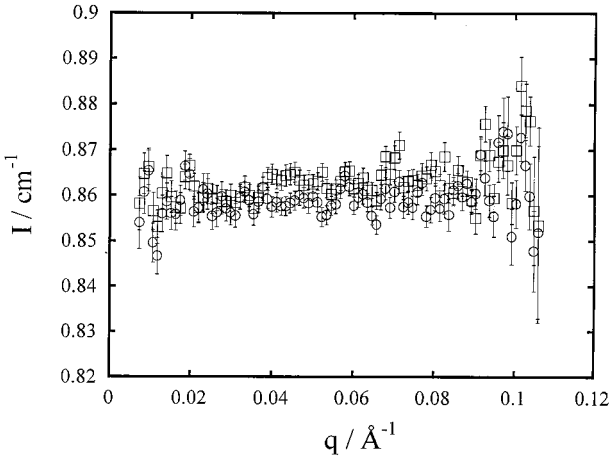

Figure 5. Plot of the absolute value of the scattering intensity of the pure matching solvent, □, and a solution of G7(H) in the matching solvent, ○. The composition of the matching solvent, composed of CD_3OH and CH_3OH, is $\phi_{match} = 0.388 \pm 0.010$; the molar volume concentration of the dendrimer solution is $c = 7 \times 10^{-5}$ mol dm^{-3}.

matching solvent with and without dendrimers. The scattering is identical for each sample with no coherent signal.

The partially labeled dendrimer G7(D) was measured in the matching solvent at the same concentration, $c = 7 \times 10^{-5}$ mol dm^{-3}. Calculation of the molar concentration was based on the theoretical molecular weight of G7(D) as 1.175×10^5 g mol^{-1}. Subtracting the scattering of the solvent from each set of dendrimer scattering data eliminates the incoherent contribution and leaves only the coherent scattering signal for the deuterated segments of the G7(D) dendrimer, i.e., only layer G6.5 of the dendrimer. The absolute value of this coherent scattering intensity is small compared to the relatively large amount of incoherent scattering due to the hydrogen present in the solution. This leads to uncertainties in the intensity values, which may not be accounted for fully by the standard deviation calculated during the circular averaging. The uncertainty in the baseline can be propagated through the calculations and slightly increases the standard deviation in the measured R_g. It is important to note that this uncertainty is correlated

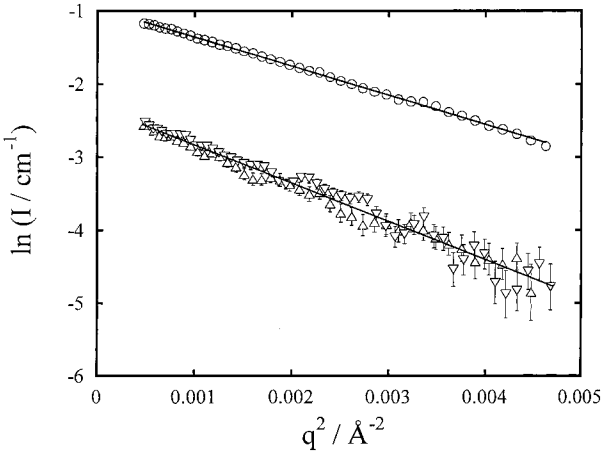

Figure 6. Guinier plot of the absolute coherent scattering intensities for G7(H) in CD_3OH (○) and for G7(D) in matching solvent, measured with the instrument NG3 (▽) and measured with the instrument NG7 (△) at NIST (all concentrations, $c = 7 \times 10^{-5}$ mol dm^{-3}). The solid lines represent the results of weighted linear least-squares fits.

in both measurements, so that deviations in the ratio of the R_g values is minimal.

To ensure that instrumental artifacts do not perturb the results, we collected two independent data sets for G7(D) in the matching solvent by measuring the solutions on both 30M SANS instruments at NIST. In addition, as described above, we used slightly different instrument parameters and reduced the data to absolute intensities using a secondary standard. Figure 6 shows the Guinier plots of the scattering of G7(D) in the matching solvent and of G7(H) in CD_3OH. The absolute values of the coherent scattering intensity of the G7-(D)-labeled segments are reproduced to high accuracy, independent of the SANS instrument and its configuration. The values of the radius of gyration are determined by weighted linear least-squares fits to the Guinier plots as shown in Figure 6 with solid lines. The radius of gyration of nonlabeled dendrimer is 34.4 ± 0.2 Å. For the deuterated segments of the partially deuterated dendrimer, the results are R_g(G7(D)) = 38.8 ± 1.2 Å and R_g(G7(D)) = 39.8 ± 1.2 Å for the data taken on NG3 and NG7, respectively (uncertainties are based on the standard deviation of the fits). We can take the average value of R_g(G7(D)) as 39.3 ± 1.0 Å for the deuterated segments of G6.5 in a G7 dendrimer. All these values are measured with solutions of a molar volume concentration of 7×10^{-5} mol dm^{-3} so it is expected that any small influence of the structure factor will be similar in each case. Therefore, the relative sizes of the R_g values is representative of the zero concentration values.

If a uniform distribution of end groups were present throughout the dendrimer, we would see the same R_g for both the labeled and the whole dendrimer. Instead, we see a clear difference between the R_g values for the labeled units and the unlabeled dendrimers. The distribution of dendrimer terminal groups is not uniform throughout the interior of the dendrimer, but rather the terminal groups are localized near an outer shell.[35]

For a more quantitative discussion we can relate the radius of gyration of a uniform density sphere to its corresponding radius, R.

$$R_g = (^3/_5)^{1/2} R_h \qquad (2)$$

For higher generation PAMAM dendrimers the uniform segment density distribution has been shown to be a good approximation.[19−24] In contrast, the radius of gyration of a spherical shell is equal to the shell radius. From R_g(G7(H)) = 34.4 ± 0.2 Å, we compute an equivalent sphere radius for the G7 dendrimer of R = 44.4 ± 0.3 Å. The deuterated segments of the G7(D) dendrimer lie at generation 6.5, giving an R_g value of 39.3 Å which is consistent with a spherical shell of an equivalent radius. This corresponds to the idealized picture of a dendrimer where most of the terminal units are distributed near the periphery of the dendrimer, with the deuterated segments of G6.5 lying within a shell of a slightly smaller radius. We take these quantitative results as demonstration that the terminal units of a high-generation PAMAM dendrimer are preferentially located at the outside of the dendrimer.

As noted in the Introduction, most simulations and theoretical approaches predict segment density distributions in which the terminal groups are dispersed throughout the interior of the dendrimer. We can provide a more quantitative comparison of our experimental results with those of the Monte Carlo simulations by Mansfield and Klushin.[7,8] For a G7 dendrimer of a spacer length corresponding to the PAMAM dendrimer, Mansfield and Klushin found the radius of gyration for the whole dendrimer of R_g(all) = 32.5 Å and a radius of gyration for the terminal groups of R_g(end) = 34.4 Å.[36] We note that the value for the size of the whole dendrimer is in reasonable agreement with our experimental result, considering that the simulation was carried out for a dendrimer with a trifunctional core. We can compute a ratio of R_g(all)/R_g(end) = 0.945 from the simulation and a ratio of R_g(all)/R_g(G6.5) = 0.88 ± 0.03 for our SANS results. The difference between the two ratios is well outside the experimental uncertainty, especially considering that the experimental ratio is calculated only for the value R_g(G6.5), whereas the simulation considered the terminal beads. The difference reflects that the simulated structures must not capture the full chemical structure of the PAMAM dendrimers. This was also noted by the authors.[7]

On the basis of a rotational-echo double-resonance study with poly(benzyl ether) (PBE) dendrons, Wooley et al.[37] conclude that the terminal groups in those structures are distributed throughout the interior of the molecules. There are several differences between our PAMAM dendrimers and the PBE dendrons that may account for the different observations. First, our study used fully dendritic high-generation dendrimers whereas Wooly et al. used lower generation dendrons with the "core" at one end of the molecule having a probe label attached. Second, the PBE have a more chemically uniform and nonpolar structure than the PAMAM dendrimers. When dissolved in polar solvents such as water or alcohol, the favorable interactions with the primary amines of the PAMAM dendrimers may lead to the tendency to maximize the solvent contacts for the terminal units, as is best achieved at the dendrimer surface. A recent publication uses Monte Carlo calculations to account for ionic effects and predicts strong effects.[38]

We expect better agreement between simulation results and theoretical approaches with the characteristics of PAMAM dendrimers when structures are used that better mimic the specific chemical interactions.

Indeed, solution studies suggest that the chemically distinct terminal units of the PAMAM dendrimers play a critical role in solubility and compatibility with their surroundings while being held in place by the highly branched interior molecular scaffolding. Thus, the PAMAM dendrimers may represent a nanomolecular structure of an inherently complex design. The present study suggests that one of the features of this design is a macromolecular species with the remarkable precision to locate its terminal units and nearly half of its monomers in the vicinity of its surface.

Conclusions

SANS experiments with partially deuterated G7 PAMAM dendrimers give a larger value of the radius of gyration of the terminal groups than of the whole dendrimer. This result is consistent with an idealized model that pictures the terminal units near the outer surface of a high-generation PAMAM dendrimer. Under the assumption of uniform internal segment density, the equivalent hard-sphere radius of the dendrimer is in agreement with the radius of gyration that was determined for the labeled segments of the final generation. Our findings differ from the predictions of computer simulations.

Acknowledgment. We are grateful to M. L. Mansfield, who provided us with additional data concerning simulations. A. Topp gratefully acknowledges the financial support by the Deutsche Forschungsgemeinschaft. This material is based upon work supported in part by the U.S. Army Research Office under Contract 35109-CH.

References and Notes

(1) Certain commercial materials and equipment are identified in this paper in order to specify adequately the experimental procedure. In no case does such identification imply recommendation by the National Institute of Standards and Technology nor does it imply that the material or equipment identified is necessarily the best available for this purpose.

(2) For reviews on the synthesis of dendrimers and dendritic macromolecules see: (a) Tomalia, D. A.; Naylor, A. M.; Goddard, W. A. *Angew. Chem., Int. Ed. Engl.* **1990**, *29*, 138. (b) Hawker, C. J.; Wooley, K. L.; Fréchet, J. M. J. *J. Chem. Soc., Perkin Trans.* **1993**, *1*, 1287. (c) Fréchet, M. J. J. *Science* **1994**, *263*, 1710. (d) Tomalia, D. A. *Adv. Mater.* **1994**, *6*, 529. (e) Issberner, J.; Moors, R.; Vögtle, F. *Angew. Chem., Int. Ed. Engl.* **1994**, *33*, 2413. (f) Voit, B. I.; Turner, S. R. *Angew. Makromol. Chem.* **1994**, *223*, 13. (g) Ardoin, N.; Astruc, D. *Bull. Soc. Chim. Fr.* **1995**, *132*, 875. (h) de Brabander, E. M. M.; Brackman, J.; Mure-Mak, M.; de Man, H.; Hogeweg, M.; Keulen, J.; Scherrenberg, R.; Coussens, B.; Mengerink, Y.; van der Wal, S. *Macromol. Symp.* **1996**, *102*, 9. (i) Fréchet, M. J. J.; Hawker, C. J.; Gitsov, I.; Leon, J. W. *J. Macromol. Sci., Pure Appl. Chem.* **1996**, *A33*, 1425.

(3) de Gennes, P. G.; Hervat, H. *J. Phys., Lett.* **1983**, *44*, L-351.

(4) Naylor, A. M.; Goddard III, W. A. *ACS Polym. Prepr. Div. Polym. Chem.* **1988**, *29*, 215.

(5) Naylor, A. M.; Goddard III, W. A.; Kiefer, G. E.; Tomalia, D. A. *J. Am. Chem. Soc.* **1989**, *111*, 2339.

(6) Lescanec, R. L.; Muthukumar, M. *Macromolecules* **1990**, *23*, 2280.

(7) Mansfield, M. L.; Klushin, L. I. *Macromolecules* **1993**, *26*, 4262.

(8) Mansfield, M. L. *Polymer* **1994**, *35*, 1827.

(9) Murat, M.; Grest, G. S. *Macromolecules* **1996**, *29*, 1278.

(10) Chen, Z. Y.; Cui, S.-M. *Macromolecules* **1996**, *29*, 7943.

(11) Carl, W. *J. Chem. Soc., Faraday Trans.* **1996**, *92*, 4154.

(12) Boris, D.; Rubinstein, M. *Macromolecules* **1996**, *29*, 7251.

(13) Tomalia, D. A.; Hall, M.; Hedstrand, D. M. *J. Am. Chem. Soc.* **1987**, *109*, 1601.

(14) Tomalia, D. A.; Hedstrand, D. M.; Wilson, L. R. *Encyclopedia of Polymer Science and Engineering*, 2nd ed.; Wiley: New York, 1990; Index Vol., pp 46−92.
(15) Caminati, G.; Turro, N. J.; Tomalia, D. A. *J. Am. Chem. Soc.* **1990**, *112*, 8515.
(16) Gopidas, K. R.; Leheny, A. R.; Caminati, G.; Turro, N. J.; Tomalia, D. A. *J. Am. Chem. Soc.* **1991**, *113*, 7335.
(17) Meltzer, A. D.; Tirrell, D. A.; Jones, A. A.; Inglefield, P. T.; Hedstrand, D. M.; Tomalia, D. A. *Macromolecules* **1992**, *25*, 4541.
(18) Meltzer, A. D.; Tirrell, D. A.; Jones, A. A.; Inglefield, P. T. *Macromolecules* **1992**, *25*, 4549.
(19) Bauer, B. J.; Hammouda, B.; Barnes, J. D.; Briber, R. M.; Tomalia, D. A. *ACS Polym. Mater. Sci. Eng. Proc.* **1994**, *71*, 704.
(20) Bauer, B. J.; Topp, A.; Prosa, T. J.; Amis, E. J.; Yin, R.; Quin, D.; Tomalia, D. A. *ACS Polym. Mater. Sci. Eng. Proc.* **1997**, *77*, 87.
(21) Prosa, T. J.; Bauer, B. J.; Amis, E. J.; Tomalia, D. A.; Scherrenberg, R. J. *J. Polym. Sci., Polym. Phys. Ed.* **1997**, *35*, 2913.
(22) Bauer, B. J.; Briber, R. M.; Hammouda, B.; Tomalia, D. A. *ACS Polym. Mater. Sci. Eng. Proc.* **1992**, *67*, 428.
(23) Bauer, B. J.; Hammouda, B.; Briber, R. M.; Tomalia, D. A. *ACS Polym. Mater. Sci. Eng. Proc.* **1994**, *71*, 342.
(24) See ref 2a and references therein for details.
(25) Values for the densities are as given in the product specification by the manufacturer; no attempt was undertaken to verify the values.
(26) Note: According to ISO 31-8, the term "molecular weight" has been replaced by "relative molecular mass," symbol M_r. Thus, if this nomenclature and notation were to be followed in this publication, one would write $M_{r,n}$ instead of the historically conventional M_n for the number-average molecular weight, with similar changes for M_w, M_z, and M_v, and it would be called the "number-average relative molecular mass". The conventional notation, rather that the ISO notation, has been employed for this publication.
(27) Prask, H. J.; Rowe, J. M.; Rush, J. J.; Schröder, I. G. J. *Res. Natl. Inst. Stand. Technol.* **1993**, *98*, 1.
(28) Hammouda, B.; Krueger, S.; Glinka, C. *J. Res. Natl. Inst. Stand. Technol.* **1993**, *98*, 31.
(29) Glinka, C. J.; Barker, J. G.; Hammouda, B.; Krueger, S.; Moyer, J. J.; Orts, W. J. *J. Appl. Crystallogr.* **1998**, *31*, 430.
(30) Note: Different instruments and configurations were used to investigate possible artifacts as described in section 3.3.
(31) *SANS Data Reduction and Imaging Software*; Cold Neutron Research Facility, NIST: Gaithersburg, MD 20899, 1996.
(32) Guinier, A.; Fournet, G. *Small Angle Scattering of X-rays*; Wiley: New York, 1955.
(33) Topp, A.; Bauer, B. J.; Prosa, T. J.; Scherrenberg, R.; Amis, E. J., to be published.
(34) Higgins, J. S.; Benoit, H. C. *Polymers and Neutron Scattering*; Oxford Universty Press: New York, 1994.
(35) Uppuluri, S.; Tomalia, D. A.; Dvornic, P. R. *ACS Polym. Mater. Sci. Eng. Proc.* **1997**, *77*, 87.
(36) Personal correspondence with M. L. Mansfield.
(37) Wooley, K. L.; Klug, C. A.; Tasaki, K. Schaefer, J. *J. Am. Chem. Soc.* **1997**, *119*, 53.
(38) Welch, P.; Muthukumar, M. *Macromolecules* **1998**, *31*, 5892.

MA990125S